JOURNAL OF APPLIED POLYMER SCIENCE VOL. 21, 2695–2709 (1977)

Kinetics of Thermal Polymerization of Shellac. V. Turbidimetric and Fractionation Studies

A. KUMAR, *Indian Lac Research Institute, Namkum, Ranchi, Bihar, India*

Synopsis

In the present investigation, the changes in precipitation of the shellac condensates with curing time have been followed turbidimetrically. The experimental data support the saturation limit law. Further, the fractionation of a polymer with low degree of polymerization has been effected by the integral method, and the relation between W_x (the weight fraction of the precipitate) and v (the volume of precipitant added) has been established. In addition, the fractions have been characterized in terms of inherent viscosity. The experimental data, which exhibit alternation behavior, have been confirmed by a number of statistical tests.

INTRODUCTION

A knowledge of molecular weight and size is essential for an understanding of the physical behavior of high polymers.[1] Generally, the polymers consist of molecules with a more or less broad range of sizes.[2] It should be pointed out that the size disparity arises from the random nature of chemical reaction and equal reactivity of the same class.[3] In heterogenous polymers, the molecular size is not sufficiently characterized by an average value.[4] Therefore, it seems indispensible to determine the distribution of molecular weights or sizes about the mean value for correlating with reaction kinetics[5] and also for tailoring polymers so as to have desired physical properties.[6] In fact, there are several methods for the determination of the molecular weight distribution function, but the turbidimetric titration is commonly used for a variety of reasons.[7] On this account, an effort has been made to determine the molecular weight distribution function turbidimetrically.

EXPERIMENTAL

Reagents. Methanol B.D.H. (Laboratory reagent). Potassium chloride—pure (Merck).

Polymerization. Dewaxed, decolorized shellac samples (dried and desiccated, 10 g each) were polymerized at 150° ± 1°C by the usual method.[8] The condensates were powdered, passed through a 40-mesh sieve, and kept in the dark prior to use.

Turbidimetric Titration. For the determination of the precipitation point, 5 ml of 1.0% polymer solution in methanol was introduced in a clean 100-ml glass-stoppered (Pyrex) conical flask suspended in a thermostated bath main-

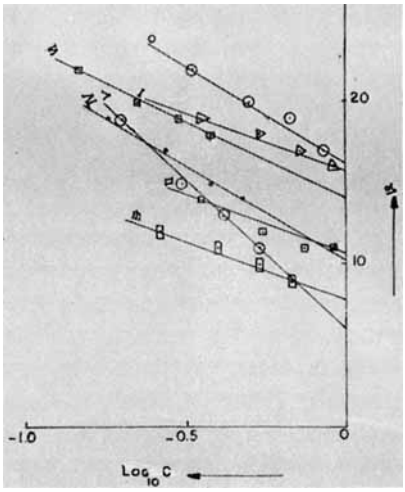

Fig. 1. Dependence of v on concentration.

tained at 35° ± 0.5°C. After the attainment of the bath temperature, the nonsolvent (water) was slowly added until a haze appeared. The amount of the nonsolvent required for the onset of precipitation (v) was calculated in terms of percentage. The precipitation points at several concentrations were determined likewise. The results are presented in Figure 1.

Isolation of Fractions. There are many methods for polymer fractionation, viz., fractional precipitation, extraction, elution, thermal diffusion, zone refining, ultrafiltration, selective absorption, Brownian diffusion, chromatography (precipitation and absorption), and turbidimetric titration. Out of all these methods, the turbidimetric titration has been used as an analytical tool.[9] The underlying principle rests on the observation that the less soluble high molecular weight polymers precipitate out first, followed by low molecular weight species.[3] The results are altered by aging or agglomeration or coagulation of the precipitate.[2] The turbidity in all these cases varies without any change in the amount of polymer precipitated. Therefore, an attempt has been made to weigh out the precipitate gravimetrically.

For the study, 5 ml 1% solution of shellac condensate designated as polymer II in methanol was charged into several thin-walled, flat-bottomed specimen tubes and corked. The nonsolvent addition was carried out in a bath thermostated at 35° ± 1°C. To the first aliquot, the amount of nonsolvent added was just sufficient to bring the solution to the verge of precipitation.

It is known that a minimum concentration of electrolyte is required for flocculation of a suspension.[10] Therefore, 0.2 g solid KCl was used to coagulate the stable suspension. After allowing to stand overnight, the material was filtered through a clean glass-sintered Pyrex crucible. The precipitate was repeatedly washed with water till free of KCl, dried under vacuum, and accurately weighed in a weighing bottle. From this amount and the initial concentration of the polymer solution, the weight fraction (W_x) of the precipitate was calculated. To the remaining aliquots, the increased amounts of nonsolvent were added, and the weight fractions of the precipitates were determined likewise. The results are contained in Table I.

TABLE I
Fractionation Data of a Typical Shellac Condensate

Fraction	V, ml	$100/(100+\upsilon)$	Weight fraction W_x	$\log W_x-(1-W_x)$	Intrinsic viscosity $[\eta]$	Cumulative intrinsic viscosity $\Sigma[\eta]$	$[\eta]/W_x$	$\log [\eta]/W_x$
a	10	0.909	0.142	−0.7812	0.08	0.08	0.56	−0.2518
b	12	0.893	0.178	−0.6645	3.10	3.18	17.42	1.2410
c	14	0.877	0.240	−0.5006	2.23	5.41	9.29	0.9680
d	16	0.862	0.284	−0.4016	0.40	5.81	1.41	0.1492
e	18	0.847	0.309	−0.3495	2.46	8.27	7.96	0.9009
f	20	0.833	0.337	−0.2939	1.47	9.74	4.36	0.6395
g	22	0.820	0.363	−0.2442	1.55	11.29	4.27	0.6304
h	24	0.806	0.397	−0.1815	2.44	13.73	6.15	0.7889
i	26	0.794	0.459	−0.0714	0.64	14.37	1.39	0.1430
j	28	0.781	0.461	−0.0679	0.71	15.08	1.54	0.1875
k	30	0.761	0.497	−0.0052	0.74	15.82	1.49	0.1732
l	32	0.758	0.523	−0.0400	0.44	16.26	0.84	−0.0757
m	40	0.714	0.577	0.1349	0.06	16.32	0.10	−0.0000
n	50	0.667	0.669	0.3056	0.90	17.22	1.34	0.1271
o	60	0.625	0.767	0.5174	0.10	17.32	0.13	−0.8861

TABLE II
Values of $f(M)$ and K as Function of Polymerization Time for Shellac Condensates Polymerized at 150°C

Polymer designation	Polymerization, time, min	K	$f(M)$
O	0	12.73	16.2
I	5	7.50	15.8
II	10	7.37	10.7
III	15	7.06	7.8
IV	20	12.00	10.2
V	25	18.00	6.0
VI	30	10.00	14.0

Viscosity Measurements. The intrinsic viscosity of each fraction was determined in methanol at 35° ± 0.5°C. The results are included in Table I.

RESULTS AN DISCUSSIONS

The saturation limit law[11] states that:

$$\upsilon = K \log C + f(M)$$

where υ is percent nonsolvent added for incipient precipitation of the polymer, C is the concentration at the precipitation point, and $f(M)$ is the function of molecular weight.

According to the above equation, the plot of υ vs log C should be a straight line. Such plots of turbidimetric data are shown in Figure 1. The value of $f(M)$ and K are given in Table II.

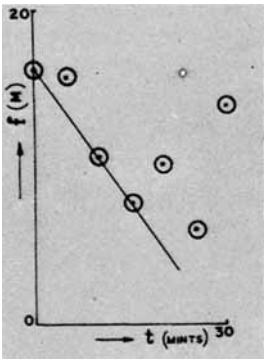

Fig. 2. Dependence of $f(M)$ on time of polymerization.

Dependence of $f(M)$ and K on Polymerization Time in the Pregelation Stage

The dependence of $f(M)$ and K on polymerization time is shown in Figures 2 and 3. Since the intermolecular reaction of the pregelation stage is of zero order,[8] it is expected that $f(M)$, being a function of molecular weight, should vary linearly with time. This is the case up to the gel point (Fig. 2). Figure 3 indicates that the parameter K, which decreases gradually with polymerization time, becomes constant at the gel point.

Dependence of $f(M)$ on Number- and Weight-Average Molecular Weights (M_n and M_w)

According to Brønsted and Schulz, the precipitation point v at constant concentration is linearly related to the reciprocal molecular weight; but Harris and Miller[12] have observed that the plot of v vs $1/M$ is not linear. They have suggested that the plot of log M vs log $f(M)$, which is nearly linear, can be used as the calibration curve for the determination of molecular weight.

More recently,[13] it has been proposed that

$$v = a \log \frac{1}{[\eta]} + b$$

This can be rewritten as

$$v = b - a \log [\eta]$$

Also, $[\eta] = KM^{\alpha}$ (Mark–Houwink–Sakurada equation). Therefore,

$$\log [\eta] = \log K + \alpha \log M$$

On substitution,

$$v = b - a \log K - a\alpha \log M$$

Let $b - a \log K = A$ and $a\alpha = B$. Then, $v = A - B \log M$. Therefore, the plot of v against log M (at constant concentration) should be a straight line. Again,

$$v = K \log C + f(M)$$

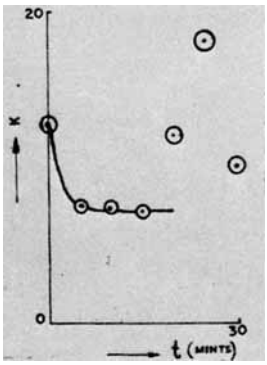

Fig. 3. Dependence of K on time of polymerization.

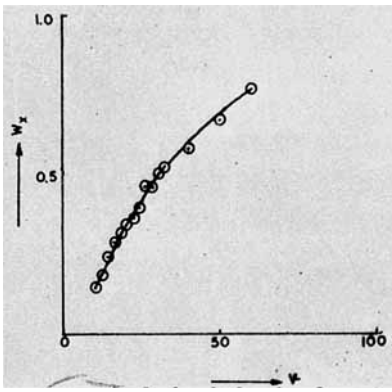

Fig. 4. Dependence of weight fraction W_x on v.

Therefore,

$$K \log C + f(M) = A' - B \log M$$

Since C is constant, we can write that $f(M) = A' - B \log M$.

If these relations hold, a plot of $f(M)$ vs $\log \overline{M}_n$ or $\log \overline{M}_w$ should be a straight line. Secondly, as M would increase, $f(M)$ would decrease. That is to say, the greater the molecular weight, the smaller would be the corresponding $f(M)$ value.

Dependence of W_x on v

The plot of the weight fraction of the polymer precipitated, W_x, against the percentage of precipitant added, v, is shown in Figure 4. A relation between W_x and v is now deduced.

Let C_0 be the initial concentration (in g/100 ml) of the shellac condensate and v be the per cent nonsolvent added for the onset of precipitation; C represents the concentration at the saturation point. Then,

$$C = \frac{100C_0}{100 + v} = \frac{C_0}{1 + v/100}$$

Suppose C_p is the amount of polymer precipitated (in g) and v be increased

to $v + dv$. Let C' (in g/100 ml) represent the concentration at the next saturation point. Then,

$$C' = \frac{100(C_0 - C_p)}{100 + v + dv} = \frac{(C_0 - C_p)}{1 + (v + dv)/100}$$

Hence,

$$\frac{C'}{C} = \frac{1 + (v/100)}{1 + (v/100) + (dv/100)} \cdot [1 - (C_p/C_0)]$$

From the saturation limit law,

$$v = K \log C + f(M)$$

or

$$\log C = \frac{v - f(M)}{K}$$

Therefore,

$$C = 10^{[v - f(M)]/K} = 10^{v/K} \times 10^{-f(M)/K}$$

If $dv \ll v$, then the solution at both dilutions v and $v + dv$ would be saturated with respect to species M_i. From the above-derived equation, it follows that

$$C' = 10^{(v+dv)/K} \times 10^{-f(M)/K}$$

Hence,

$$\frac{C'}{C} = 10^{dv/K}$$

On equating the two C'/C terms, one obtains

$$1 - (C_p/C_0) = 10^{dv/K} \times \frac{1 + (v/100) + (dv/100)}{1 + (v/100)}$$

$$= 10^{dv/K} \times \left[1 + \frac{dv}{(100 + v)}\right]$$

or

$$C_p/C_0 = 1 - 10^{dv/K} \times [1 + dv/(100 + v)]$$

$$= 1 - 10^{dv/K} - \frac{dv}{100 + v} \times 10^{dv/K}$$

If dv is experimentally kept constant, then

$$C_p/C_0 = A - \frac{B}{100 + v}$$

The term C_p/C_0 is the weight fraction of the polymer precipitated, i.e., W_x. Therefore,

$$W_x = A - \frac{B}{100 + v}$$

Evidently, a plot of W_x against $1/(100 + v)$ would be a straight line. Such a plot

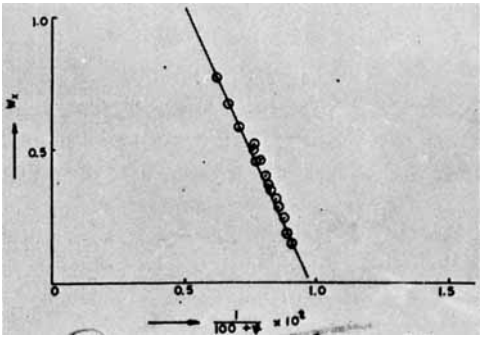

Fig. 5. Relation between W_x on v.

of the fractionation data is shown in Figure 5, which is strictly linear. This supports the above relationship showing the dependence of W_x on v.

Basic Theories of Precipitation

For the precipitation to occur, the solution must be supersaturated with respect to the solute so that the metastable state of supersaturation may revert back to the stable state by the release of excess solute as a precipitate.[14] There are two stages involved in the initial formation of a precipitate: (i) the induction period required for the first nuclei to form, and (ii) the period of crystal growth until a stable state is reached.[14]

The nucleation begins when the concentration of different ions reaches values equal to or higher than those of the solubility product.[15] In the beginning, the nuclei grow rapidly, diminishing supersaturation and solubility, but subsequent growth is slower.[14] The rate of nucleation[16] has been expressed as

$$R = Ae^{-\Delta G/kT}$$

where ΔG is the free energy of activation, k is the Boltzmann constant, T is absolute temperature, and A represents the frequency factor. Very recently, the phenomenon of nucleation has been discussed in terms of heterophase fluctuations[17] called embryos, that is, minute, unstable, temporary aggregations constantly forming and disappearing.

The energy required for embryo growth increases only up to a critical size and then falls off rapidly with increasing particle diameter. The embryos of critical size are called three-dimensional nuclei.[17] As soon as one or more stable nuclei are formed, the crystallization begins. It stops when the potential of the liquid phase equals that of the solid phase.[17]

The theories of crystal growth are now discussed. According to the migration theory,[18] the incoming unit is not immediately incorporated in the growing phase even if it has arrived on the site by diffusion. It sticks only to a place of stronger attachment, viz., edge, corner, surface, hole, etc. On the other hand, according to the spiral growth theory,[18] the surface of most crystals contains dislocations with a screw component, and the spiral growth takes place at such dislocated sites resulting from surface nucleation, high supersaturation, incorporated or absorbed impurity, mechanical stress, fluctuations in temperature, etc.

The crystals can also develop by heterogeneous nucleation at the surface of

the suspended insoluble impurity or on the walls of the container or at the surface of a liquid or at a liquid–liquid boundary.[17] It should be pointed out that the ratio of crystal growth to nucleation rate is a measure of crystal size.[16] The larger the ratio, the coarser the product. Secondly, the rate of crystal growth at lower concentration is diffusion controlled, and the resulting crystals are reasonably perfect.[14] This is one of the reasons why a polymer solution of less than 1% concentration is chosen for the fractionation study.

In the light of the above discussion, it can be inferred that on the gradual addition of a nonsolvent to the shellac condensate solution, a metastable state is created which, by way of nucleation and crystal growth, gives the cloudy precipitate.

Distribution of Molecular Species

The molecular weight of a precipitate depends on the nonsolvent/solvent ratio.[19] The distribution of molecules[20] between the dilute solution phase and the precipitate phase is dependent on the chain length (i.e., molecular weight). According to Spencer,[21] the polymers with molecular weights above M_{solid} remain in the precipitate phase, and polymers with molecular weights below M_{solution} pervade the solution phase. Brønsted and Schulz[22] have proposed the following formula for the distribution of molecular species into two phases:

$$v_x'/v_x = e^{\sigma x}$$

where v_x' and v_x are the volume fractions of polymer of the degree x of polymerization in the precipitate and dilute solution phase, respectively, and σ is a complex function of the Flory–Huggins interaction constant, the molecular weight distribution, and the concentration. Schulz[23] has also suggested another formula based on the relative potential energy of a chain molecule in the solution and the precipitate phase. That is,

$$C_i''/C_i' = \exp \frac{rE}{RT}$$

where rE represents the gain of energy on transferring a polymer molecule of chain length r from one phase to the other. The conditions of phase separation[24] have been also predicted in terms of thermodynamic activity.

The plot of log $(W_x/1 - W_x)$ against $[\eta]$, which is a function of chain length r, is shown in Figure 6. Except for a few scatters, the points fall upon two straight lines in support to the Schulz's theory and the theory of alternation as discussed later.

Characterization of Fractions

A number of methods for determining molecular weight can be employed for the characterization of the functions. Generally, the density, index of refraction, and inherent viscosity are used for this purpose.

The density of a polymer is an index of the region of primary valence in the lattices[25] and does not vary significantly with $\overline{M}_n$. But this method has limited scope. The plots of n_D vs $(\overline{M}_n)^{-1}$ are undoubtedly straight lines,[26] but the changes in n_D with M_n are very small. However, on account of the direct dependence on M and ease of determination, the inherent viscosity is commonly

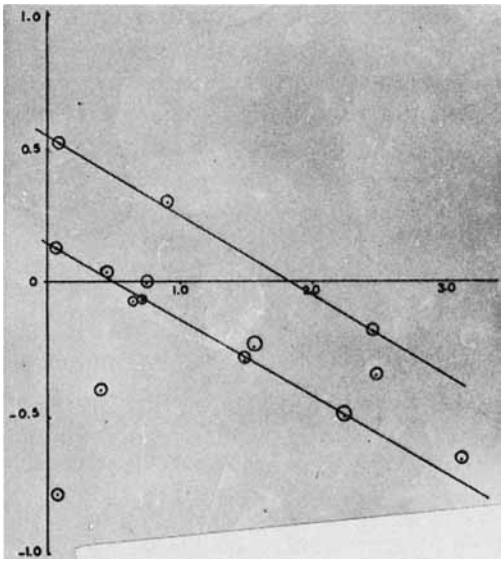

Fig. 6. Plot of log $W_x/(1 - W_x)$ vs $[\eta]$.

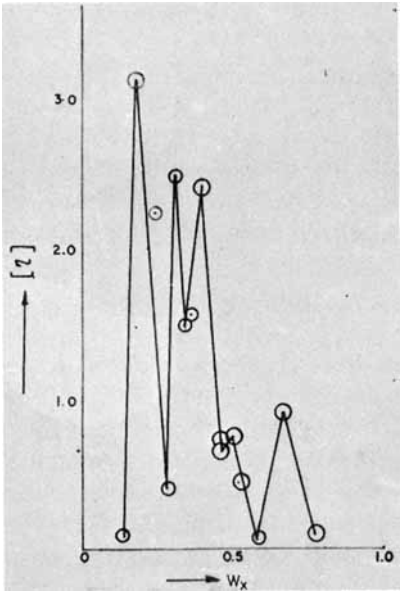

Fig. 7. Relation between W_x and $[\eta]$.

used for the characterization of the polymers. In the present case, the fractions have been characterized by inherent viscosity. The plot of W_x vs $[\eta]$ is shown in Figure 7. The graph contains multiple peaks and thus represents a multimodal distribution.

Molecular Weight and Distribution Function

For the determination of molecular weight distribution function, the polymer is dissolved in a suitable solvent at sufficiently dilute concentration and frac-

tionated either by the repetitive addition of nonsolvent or by lowering the temperature of the solution. Then, the cumulative weights of the fractions are plotted against their molecular weights so as to define the integral weight distribution function. In actual practice, one half of the weight percent of the fraction plus the sum of the weight percentages of the preceding fraction is plotted versus the molecular weight of the ith fraction. The differential weight distribution are obtained by graphic differential of the integral curve. The procedure assumes that each fraction has a symmetric molecular weight distribution, and the overlapping of fractions does not take place to any appreciable extent.

Tung[27] has proposed the following equation for correlating the integral molecular-weight distribution:

$$I(M) = I - \exp(-aM^b)$$

where a and b are two adjustable parameters. The corresponding differential distribution is

$$W(M) = abM^{b-1} \exp(-aM^b)$$

Wassleu has proposed the following distribution function:

$$I(M) = \frac{1}{B\sqrt{\pi}} \int_{-\alpha}^{\ln M} \exp\left[-1/B^2 \cdot \ln^2 \frac{M}{M_0}\right] d \log M$$

where B and M_0 are two adjustable parameters. The corresponding differential distribution function is

$$W(M) = \frac{1}{B\sqrt{\pi}} \cdot \frac{1}{M} \exp\left[-1/B^2 \cdot \ln^2 \frac{M}{M_0}\right]$$

Recently, a method[28] of directly determining the differential distribution has been developed. The method entails the construction of a triangle of $dw/d(\log M)$ vs $\log M$ with three parameters representing three characteristic molecular weights.

In the integral method, the fractions are collected by the addition of the increased amounts of nonsolvent to a given volume of the polymer solution. The technique has been developed by Billmeyer and Stockmeyer[29] and others. From the weight-average molecular weight and mass of the fraction, the distribution width is calculated in terms of a parameter H which, in turn, is related to another parameter of the distribution width such as $\overline{M}_w/\overline{M}_n$. It should be added that the distribution curves at small conversion permit the determination of the true forms of the distribution functions.[30]

Statistical Analysis of Fractionation Data

An inspection of Figure 7 shows that it is difficult to offer an explanation for such a disposition of data. However, an attempt has been made to confirm the experimental data by a number of statistical tests. There are several statistical methods[31] for displaying the distribution data diagrammatically (i.e., the construction of histogram or polygon). The most common and convenient method is the cumulative frequency diagram. In this method, a number of intervals, usually of equal lengths, are marked on a horizontal axis. The midpoint of each

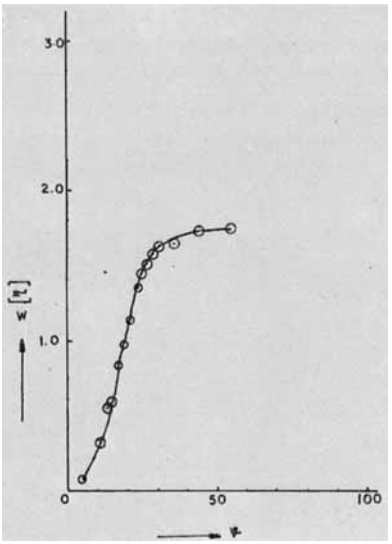

Fig. 8. Cumulative inherent viscosity polygon.

interval is labeled with the value of the variate to which it corresponds. Then, an ordinate measuring the "accumulated" frequency (up to and including that value of the variate) is erected at the midpoint of each such interval and the upper endpoints of the neighboring ordinates are joined. The resulting figure represents the cumulative frequency polygon.

The cumulative inherent viscosity polygon is shown in Figure 8. The S-shaped graph justifies the viscosity data. Apart from this, a simple mathematical tool has been designed to test the validity of the fractionation data.

The weight-average intrinsic viscosity of the aliquots, obtained on admixing two, three, four, etc., fractions together, can be given by the equation of the type

$$[\eta]_w = \frac{\Sigma W_x[\eta]}{W_x}$$

The value of $[\eta]_w$ together with the number of fractions admixed (n_f) are contained in Table III. The plot of $[\eta]_w$ against n_f is shown in Figure 9. The linearity of the plot provides additional evidence in favor of the generated fractionation data.

The Variation of $[\eta]$ with W_x

The physicochemical properties of the fatty acids, when plotted against their carbon number, exhibit alternation.[32] Moreover, it has been found that the experimental points fall on two smooth curves corresponding to even and odd number of carbon atoms. The situation bears a close analogy to the present case.

As can be seen, the upper and lower points in Figure 10 tend to fall on two different curves. Therefore, the incorporation of even and odd numbers of carbon atoms into these fractions may be responsible for the alternation of in-

TABLE III
Weight-Average Inherent Viscosities $[\eta]_w$ and Fraction Numbers n_f of the Hypothetical Admixtures in Question

n_f	$[\eta]_w$
1	0.8
2	1.78
3	1.96
4	1.43
5	1.71
6	1.66
7	1.63
8	1.78
9	1.58
10	1.46
11	1.36
12	1.24
13	1.17
14	1.13
15	1.01

herent viscosity. Further, it has been found that

$$\log \frac{[\eta]}{W_x} = a + b[\eta]$$

A plot of log $([\eta]/W_x)$ vs $[\eta]$ is shown in Figure 11. All points (except a few) fall on two straight lines. This provides an additional proof in favor of the data and treatment of the subject matter.

CONCLUSIONS

The following conclusions can be drawn from the foregoing paragraphs.

The solubility is depressed on the addition of a nonsolvent, and upon the attainment of supersaturation, the precipitation occurs.

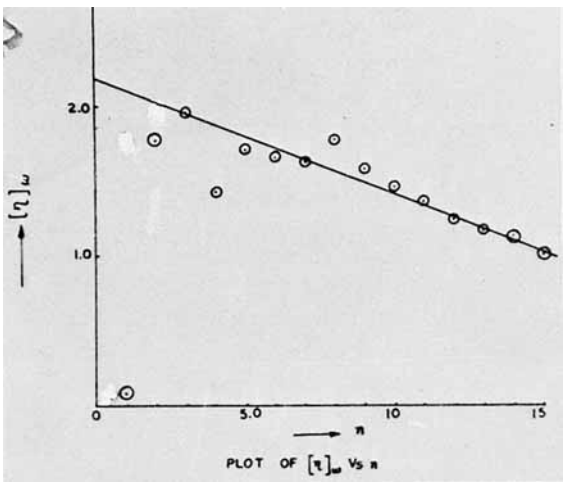

Fig. 9. Plot of $[\eta]_w$ vs n_f.

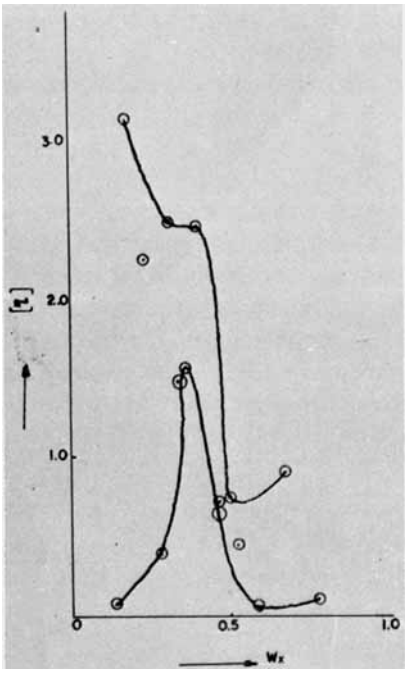

Fig. 10. Plot of $[\eta]$ vs W_x.

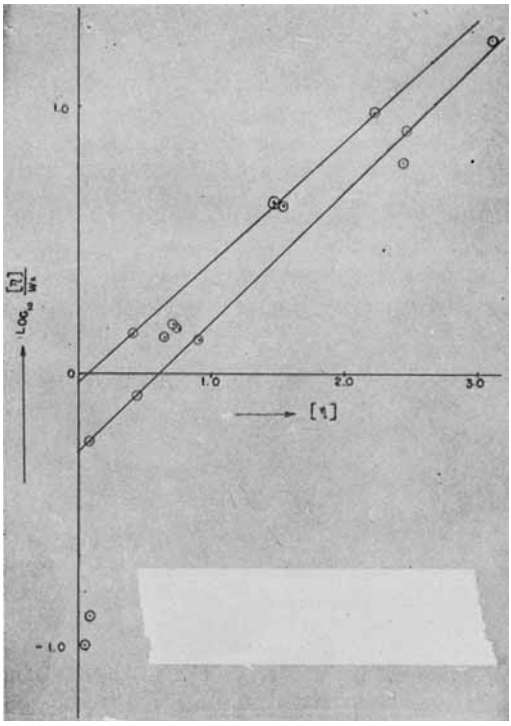

Fig. 11. Plot of log $[\eta]/W_x$ vs $[\eta]$.

The volume of the nonsolvent required for the incipient precipitation depends on the concentration of the polymer solution.

The weight fraction of the precipitate depends on the volume of the nonsolvent added.

The inherent viscosities of the fractions exhibit a natural mode of distribution.

The manifestation of alternation in the present instance proves the presence of even and odd numbers of carbon atoms in the isolated fractions.

It is suggested that the integral method of fractionation allows the tailoring of the polymer molecules in accordance with the chain length suitable for enduse. On the other hand, the differential method of fractionation facilitates identification of macromolecular species of different chain lengths present in the polymerization product.

The author wishes to thank Professor S. R. Palit, D.Sc., F.R.I.C., F.N.A., for valuable suggestions and to Dr. J. N. Chatterjea, D.Sc., D.Phil., F.R.As.C., F.R.I.C., F.N.A., for kind permission to publish this paper.

References

1. D. J. Harmon, *J. Polym. Sci. C,* **8,** 243 (1965).
2. J. H. Badley, *J. Polym. Sci. C,* **8,** 305 (1965).
3. G. M. Guzman, *Progress in High Polymers,* Vol. I, Heywood and Company, London, 1961, pp. 115–183.
4. H. Campbell and P. Johnson, *Trans. Faraday Soc.,* **XL** (6), 221 (1944).
5. A. S. Kenyon, I. O. Salyer, J. E. Kurz, and D. R. Brown, *J. Polym. Sci. C,* **8,** 205 (1965).
6. F. W. Billmeyer, Jr., *J. Polym. Sci. C,* **8,** 161 (1965).
7. R. W. Hall, *Techniques of Polymer Characterization,* Butterworth, London, 1959, pp. 53–58.
8. A. Kumar, *J. Appl. Polym. Sci.,* **8,** 1186 (1964).
9. N. S. Schneider, *J. Polym. Sci. C,* **8,** 179 (1965).
10. S. Ghosh, Presidential Address, Section of Physical Sciences, The National Academy of Sciences, India, Twenty-eighth Annual Session, Agra, Feb. 6–8, 1959.
11. D. R. Morey and J. W. Tamblyn, *J. Appl. Phys.,* **16,** 419 (1945).
12. I. Harris and R. G. J. Miller, *J. Polym. Sci.,* **7,** 377 (1951).
13. S. Tanaka, A. Nakamura, and H. Morikawa, *Makromol. Chem.,* **85,** 164 (1965).
14. E. W. Berg, *Physical and Chemical Methods of Separation,* McGraw-Hill, New York, 1963, pp. 250–295.
15. J. A. Palermo and G. F. Bennett, *Ind. Eng. Chem.,* **57,** 58 (1965).
16. D. B. Wilson, *Chem. Eng.,* 119 (1965).
17. R. S. Tipson, *Technique of Organic Chemistry,* Vol. III, Part I, Interscience, New York, 1956, Chap. III, pp. 395–414.
18. R. S. Tipson, *Anal. Chem.,* **37,** 26A (1965).
19. H. Campbell and P. Johnson, *Trans. Faraday Soc.,* **XL,** 223 (1944).
20. R. L. Scott, *Ind. Eng. Chem.,* **45,** 2532 (1953).
21. R. S. Spenser, *J. Polym. Sci.,* **3,** 606 (1948).
22. R. W. Hall, *Techniques of Polymer Characterization,* Butterworth, London, 1959, p. 20.
23. H. Tompa, *Polymer Solutions,* Butterworth, London, 1956, pp. 219–232.
24. C. M. Conrad, *Ind. Eng. Chem.,* **45,** 2511 (1953).
25. H. Mark, *Physical Chemistry of High Polymeric Systems,* Interscience, New York, 1940, p. 131.
26. J. D. Ingham and D. D. Lawson, *J. Polym. Sci.,* **A3,** 2707 (1965).
27. L. H. Tung, *High Polymers,* Vol. XX, Wiley-Interscience, New York, 1965, pp. 513–575.
28. F. Rodriguez and O. K. Clark, *Ind. Eng. Chem.,* **57,** 13 (Nov. 1965).
29. F. W. Billmeyer, Jr. and W. H. Stockmayer, *J. Polym. Sci.,* **V,** 121 (1950).

30. E. F. G. Herington, *Trans. Faraday Soc.*, **XL,** 237 (1944).
31. R. Goodman, *Teach Yourself Statistics,* The English Language Book Society and the English University Press, London, 1965, pp. 21–26.
32. A. W. Ralston, *Fatty Acids and Their Derivatives,* Wiley, New York, 1948, pp. 322–395.

Received September 19, 1975
Revised August 27, 1976